### **Article**



# The Role of Noncognate Sites in the 1D Search Mechanism of EcoRI

Sadie C. Piatt, 1 Joseph J. Loparo, 2,\* and Allen C. Price 1,\*

<sup>1</sup>Department of Chemistry and Physics, Emmanuel College, Boston, Massachusetts and <sup>2</sup>Department of Biological Chemistry and Molecular Pharmacology, Harvard Medical School, Boston, Massachusetts

ABSTRACT A one-dimensional (1D) search is an essential step in DNA target recognition. Theoretical studies have suggested that the sequence dependence of 1D diffusion can help resolve the competing demands of a fast search and high target affinity, a conflict known as the speed-selectivity paradox. The resolution requires that the diffusion energy landscape is correlated with the underlying specific binding energies. In this work, we report observations of a 1D search by quantum dot-labeled EcoRI. Our data supports the view that proteins search DNA via rotation-coupled sliding over a corrugated energy landscape. We observed that whereas EcoRI primarily slides along DNA at low salt concentrations, at higher concentrations, its diffusion is a combination of sliding and hopping. We also observed long-lived pauses at genomic star sites, which differ by a single nucleotide from the target sequence. To reconcile these observations with prior biochemical and structural data, we propose a model of search in which the protein slides over a sequence-independent energy landscape during fast search but rapidly interconverts with a "hemispecific" binding mode in which a half site is probed. This half site interaction stabilizes the transition to a fully specific mode of binding, which can then lead to target recognition.

SIGNIFICANCE We show that a model that includes both hopping and sliding can explain quantitatively the salt dependence of the diffusion of EcoRI. We quantify the separate contributions of sliding and hopping. Furthermore, we show that the theory of rotational coupling in a rough energy landscape can explain the sliding diffusion coefficient of EcoRI. We also observed pausing in the one-dimensional search and show that these pause sites map onto genomic star sites. We develop a model of one-dimensional search that includes a hemispecific binding mode that can explain the role of these pauses in the search strategy.

### INTRODUCTION

Many site-specific DNA-binding proteins perform one-dimensional (1D) diffusive scans after encountering nonspecific DNA. This idea not only explains biochemical data from several systems (1–3) but has also been directly verified in many cases through single molecule tracking of LacI (4), Rad51 (5), hOGG1 (6), p53 (7) as well as EcoRV (8). Studies of p53 (9) and zinc finger proteins (10) show that mechanisms of a 1D search can vary, requiring distinct intermediates for a rapid and accurate search. Type II restriction endonucleases (2REs) were among the first DNA binding proteins to show a 1D search (11) and remain ideal model systems for the study of the DNA target search (12)

Submitted October 15, 2018, and accepted for publication April 29, 2019. \*Correspondence: joseph\_loparo@hms.harvard.edu or priceal@emmanuel.edu

Editor: Antoine van Oijen.

https://doi.org/10.1016/j.bpj.2019.04.035

© 2019 Biophysical Society.

as well as site-specific DNA cleavage (13). Although significant structural and biochemical data exist for this class of enzymes, the mechanisms of 1D search by 2REs are poorly understood (14).

Two microscopic mechanisms have been proposed to contribute to the 1D search (15). In sliding, the protein remains in contact with the DNA helix, often rotating as it moves. Protein translocation steps involve moving to an adjacent nonspecific binding site without ion recondensation onto the DNA backbone, implying that the rate of diffusion should have little dependence on the salt concentration. Diffusion coefficients independent of salt concentration have been observed for hOGG1 (6) and T7 RNA polymerase (RNAP) (16), consistent with a sliding mechanism. This mechanism can produce thorough searches because every site in the protein's path is visited. In hopping, the protein dissociates from the DNA, allowing ion recondensation. Because of recurrence (revisiting the DNA), there is a significant probability the protein will rebind at a nearby site.



Hopping, in contrast to sliding, can produce highly transparent paths (i.e., although the displacement along the DNA may be large, only a small fraction of the nonspecific sites will be visited) (17). This type of target search can be termed "noncompact" in contrast to compact exploration, in which a highly redundant search thoroughly explores all possible sites (18). Because of the strong salt dependence of the nonspecific off rate, the balance between sliding and hopping will depend strongly on salt, and 1D searches that combine sliding and hopping will have salt-dependent diffusion coefficients. Such salt-dependent diffusion coefficients have been observed for EcoRV (8) and UL42 (19), implying that hopping contributes to the search under the buffer conditions used in those studies.

To maintain contact with nonspecific binding sites, a protein translocating along DNA must often rotate to follow the helical backbone. Theoretical analyses have shown that this significantly reduces the 1D diffusion coefficient relative to the three-dimensional constant (20,21). Single molecule tracking experiments have obtained 1D diffusion coefficients several orders of magnitude ( $10^3$ – $10^4$ ) lower than the three-dimensional constants (22). In addition, the coupling of rotation and diffusive translocation has been observed for RNAP (23). However, the rotational coupling is insufficient to explain the magnitude of the observed reduction in diffusion rate. The remaining reduction is attributed to energy barriers between nonspecific sites and to randomness in the sliding energy surface, typically of the order of 1-2 k<sub>B</sub>T (6–8).

Rapid search requires a relatively smooth energy landscape with low barriers to translocation. However, target recognition complexes typically show extensive structural rearrangements, indicating substantial barriers to specific association (14). Clearly, testing each potential binding site using the recognition conformation would significantly slow the 1D search. This conflict between the need for high affinity specific recognition and rapid diffusion has been referred to as the speed-stability paradox (24). Although the existence of this paradox has been questioned (25), models have been developed to explain how proteins can overcome this conflict (24,26). These models assume that the protein exists in at least two conformations: a search mode, expected to participate only weakly in sequence-specific interactions and which can diffuse quickly along the DNA, and a recognition mode, in which the protein adopts a conformation close to its specific binding configuration and is therefore inconsistent with rapid sliding. A key component of these models is "kinetic preselection." The sliding energy surface over which the search conformation diffuses is correlated with the highly sequence-specific energy landscape of the recognition mode. Hence, the diffusing protein spends longer periods of time at sites with a higher probability of being the target, reducing the time wasted probing unproductive sites. Such models have been applied to both p53 (9) and zinc finger proteins (10).

2REs comprise an excellent class of proteins for study of the DNA target search. Cleaving DNA at specific sites four to six basepairs in length, 2REs are a component of the bacterial innate immune system and are typically dimeric in structure. Structures of 2REs in complex with DNA have provided insight into the nature of the intermediates involved in the 1D search. The recognition complex of EcoRI with cognate DNA demonstrates extensive specific interactions via a recognition loop that extends down into the major groove (27). Although complexes of EcoRI with noncognate DNA have remained elusive, the related endonucleases, BamHI and BstYI, have yielded to crystallographic analysis (28,29). Both of these proteins approach DNA from the major groove and cleave double-stranded DNA leaving 5' overhangs as EcoRI does. As in the case of EcoRI, the cognate recognition complexes show significant specific interactions between DNA and recognition loops that enter the major groove. In contrast, the structures of BamHI and BstYI in complex with noncognate DNA (star sites that differ in a single basepair from the target sequence) show the proteins in a more open conformation, with quaternary rearrangements resulting in a wider DNA binding cleft. In the nonspecific complex, BamHI binds DNA symmetrically and does not protrude into the major groove, making no base-specific contacts. On the other hand, BstYI binds in an asymmetric manner, rotated to bring the recognition loop of one monomer into the major groove, in which it can make base-specific interactions with the cognate half site (a binding mode termed "hemispecific" by the authors of (29)). The opposing monomer, rotated away from the major groove, does not make any specific contacts with the noncognate half site. Whether these two nonspecific binding modes represent true intermediates along the 1D search pathway remains an open question.

In this article, we report our measurements of the 1D search of EcoRI along nonspecific DNA. Using total internal reflection fluorescence imaging of a QD-labeled protein, we observed 1D diffusion as well as pausing of the endonuclease on flow-stretched  $\lambda$  DNA. Using the sliding diffusion coefficient, we determined that the average energy barrier to translocation was similar to that measured for other DNA binding proteins. The diffusion coefficient increased with the salt concentration, demonstrating that the protein diffuses via sliding and hopping. Finally, we integrate our observations of pausing with existing biochemical and structural data on the 1D search by 2REs to propose a model in which the protein first identifies half cognate sites before the transition to a full recognition complex in which the entire target sequence is probed.

### **MATERIALS AND METHODS**

### **Data collection**

The conjugation of 6x-His Tag antibody (Thermo Fisher Scientific, Waltham, MA) to 605 nm QDs was carried out using a Thermo Fisher Scientific

SiteClick Qdot 605 Antibody Labeling Kit following the manufacturer's instructions. The purification of  $\rm EcoRI^{E111Q}$  protein, the functionalization of glass coverslips, the preparation of flow cells, and the preparation and labeling of biotinylated \( \lambda \) DNA with QDs were carried out as described in Graham et al. (30). In forming the quantum dot (QD)-labeled EcoRI<sup>E11Q</sup> protein, the incubation concentration was 20 nM antibody-conjugated QD and 20 nM EcoRI<sup>E111Q</sup>. Briefly, a flow cell was constructed with a coverslip functionalized with a mixture of polyethylene glycol and polyethylene glycol-biotin. A linear channel 1.8 mm wide and 120 µm high was cut out of double-sided tape (620001; Grace Bio-Labs, Bend, OR) and sandwiched between the coverslip and a quartz slide. The surface of the flow cell was coated with streptavidin, washed, and incubated with EcoRI<sup>E111Q</sup> QD-labeled  $\lambda$  DNA for ~30 min or until tethers could be clearly seen. During data collection, the flow cell was washed with 50 pM QD-labeled protein in 10 mM Tris (pH 8.0), 30–150 mM NaCl, 0.5 mM MgCl<sub>2</sub>, and 200  $\mu$ g/mL bovine serum albumin (buffer A). To doubly tether DNA, unbound  $\lambda$  DNA was washed out at 50  $\mu$ L/min with 120  $\mu$ L of buffer A. Then, 500  $\mu$ L of 100 nM biotinylated complementary oligo for the free end of the DNA (GGG-CGG-CGA-CCT-Biotin-3') was flowed in at 100 µL/min. Immediately after, the channel was washed with 240  $\mu$ L of buffer A at 100  $\mu$ L/min. Labeled proteins were imaged with a home-built through-objective total internal reflection fluorescence microscope using 532 nm excitation (Sapphire 532-75; Coherent, Santa Clara, CA). Details of the microscope and its alignment can be found in Graham et al. (30). Video data was collected at 30 fps for 120 s for salt concentrations 70 mM and above and at 1 fps for 1200 s for salt concentrations 60 mM and below.

### Data analysis

The region of the DNAs free of specifically bound proteins were identified as regions of interest for nonspecific sliding events. Tracking of proteins in the regions of interest was completed using the ImageJ plugin, Fiji Track-Mate (https://imagej.net/TrackMate). Examples of tracks are shown in Fig. S1. Custom Python code (available on request) was used to correct for finite extension of DNA, analyze mean-squared deviation (MSD), and perform linear fits to determine diffusion coefficients.

The distribution of diffusion coefficients showed a peak near zero due to paused proteins. A cutoff value of  $0.13 \times 10^{-3}~\mu m^2/s$  separated this peak from the distribution of diffusing proteins. All trajectories with a coefficient less than this cutoff were classified as paused, whereas those with a value larger than this were classified as diffusing. In cases in which pausing and diffusion were both present, the trajectory was split. Only trajectories with diffusion coefficients above the cutoff were included in calculating  $D_1$ . The mean distance of paused proteins from specifically bound EcoRIs was used to locate the pause sites in the  $\lambda$  genome. Data on numbers of replicates and events recorded at each condition is shown in Table S1. To determine the drift speed of the proteins, the slope of the longitudinal trajectories was determined by linear least-squares regression (Fig. S2). Drift speeds at each salt concentration from 30 to 90 mM were determined (Fig. S3). Drift speeds at 120 and 150 mM were not well determined because of the short interaction time.

We quantified the similarity of the observed distribution of pause sites and the genomic distribution of star sites by first binning the locations and then calculating the Pearson correlation coefficient for the resulting distributions. The correlation was 0.69. To determine the statistical significance of this correlation, we calculated a p value using the following procedure. We defined the p value to be the probability of obtaining a correlation at least as high as the observed correlation, given a random probability density of pause sites. A Monte Carlo algorithm simulated sets of random pause locations. These randomly generated locations were then binned, and the resulting distribution was compared to that of the genomic star sites. The genomic star site distribution was determined using the star sites GAATTT, GAAGTC, GAATTA, and GAACTC, which were the four most frequent star sites cleaved by EcoRI in a whole genome study (31). Randomly generated distributions that had a Pearson correlation coefficient

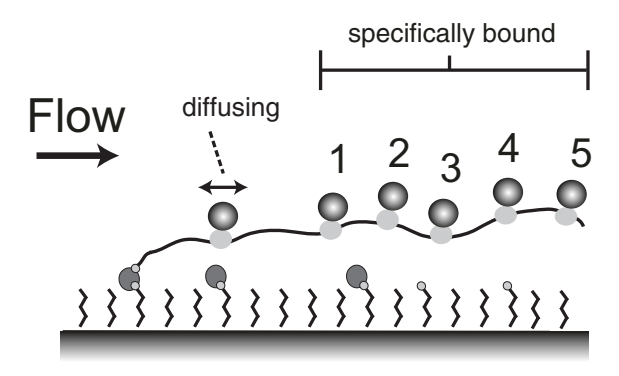
of at least 0.69 when compared with the genomic star site distribution were counted as similar. A total of  $5 \times 10^7$  simulations were performed.

### **RESULTS**

To characterize the 1D search mechanisms of EcoRI, we imaged single QD-labeled, catalytically inactive EcoRI (EcoRI<sup>E111Q</sup>) interacting with flow-stretched  $\lambda$  DNAs (Fig. 1).  $\lambda$  DNA contains five cognate EcoRI sites in the last 27 kbp. The DNA was tethered to the flow cell surface through the 5' end so that the first 21 kbp, which lack cognate sites, were located adjacent to the tether site. Nonspecific DNA interactions were analyzed by restricting analysis to events on the first 43% (lacking cognate sites) of the DNA.

We preincubated DNAs with QD-labeled EcoRI<sup>E111Q</sup> to label the five cognate sites after DNA tethering. The labeled cognate sites remained identifiable throughout data collection and served two important functions. First, they allowed for the rapid identification of tethered DNAs in a field of view. Second, they functioned as fiduciary markers that enabled us to determine the absolute location of any free EcoRI<sup>E111Q</sup> interacting nonspecifically with the DNA.

We observed nonspecific binding of EcoRI<sup>E111Q</sup> to both doubly tethered DNAs in the absence of flow as well as to singly tethered DNAs elongated under flow. A relatively low concentration of labeled EcoRI (50 pM) was necessary to reduce the background. Reducing the concentration further resulted in very few events. Even at this low concentration, under zero flow conditions, we had difficulty distinguishing nonspecifically bound proteins diffusing on the doubly tethered DNA from free proteins diffusing near the



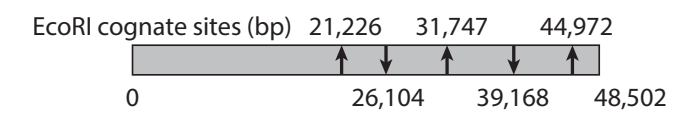
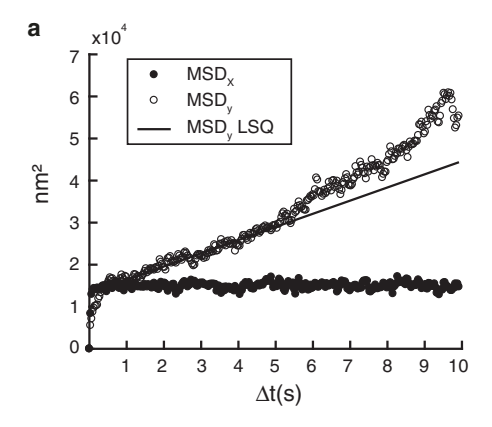


FIGURE 1 Experimental design.  $\lambda$  DNA is tethered to a glass surface via a biotin-streptavidin link and stretched by flow. QD-labeled EcoRI<sup>E111Q</sup> is bound specifically to five approximately equally spaced cognate sites on the free end of the molecule (indicated by *arrows* in the genomic map below the diagram of the experiment). Nonspecifically bound EcoRI<sup>E111Q</sup> (on *left*) is free to diffuse along the DNA.

DNA. Applying low flow (25  $\mu$ L/min) eliminated the freely diffusing proteins. Because the extension at this flow rate was 66% (see below), double tethering was unnecessary. Therefore, the results we report here are from measurements of the singly tethered DNAs under low flow conditions.

Accurate positions of the labeled proteins were determined by fitting Gaussian intensity profiles to the diffraction-limited images of EcoRI<sup>E111Q</sup>. Absolute locations in the  $\lambda$  genome were determined by measuring the distance to the labeled specific sites and correcting for the extension of the DNA. To determine the DNA extension, we made use of our previous work studying the dynamics of singly tethered DNAs in shear flow (32). In that work, we showed that the extension of the DNA is completely determined by the Weissenberg number (Wi). The Wi is a dimensionless parameter that completely characterizes the dynamics of singly tethered polymers under shear flow (33). It is equal to the ratio of the rate of shear to the relaxation rate of the polymer chain. Using the methods described in (32), we calculated Wi = 19 for our channel geometry and flow rate. We previously showed that at Wi = 19, the extension of QD-labeled λ DNA is 66% and is relatively constant from the tether point out to the second QD (32). We next experimentally measured the extension using position measurements of QDs 1 and 2 and found the extension to be 66 ± 7%, in agreement with our calculation using the Wi. All the nonspecific interactions we report in the current work were observed in the region between the tether point and the first QD, corresponding to a contour length of around 7  $\mu$ m of DNA. All data are corrected for the uniform extension of 66%.

In many cases, we observed 1D diffusion of EcoRI on  $\lambda$ DNA. An example of a diffusing trajectory is shown in Fig. 2 A. To further analyze the motion, we calculated the MSD of the longitudinal coordinate (along the DNA) as a function of the time interval. The MSDs (Fig. 3 A) displayed a linear dependence on time with a small fast component with a rise time of a few milliseconds. The transverse coordinate (perpendicular to the DNA and parallel to the tethering surface) showed constrained motion, consistent with a protein moving along a flow-stretched DNA. The MSDs



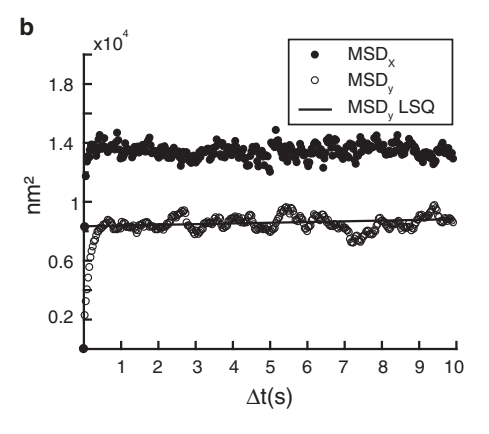


FIGURE 3 MSD plots of (a) freely diffusing and (b) paused molecules in the transverse (x) and longitudinal (y) directions. In (a), the initial slope (t < 5 s) of the MSD in the longitudinal coordinate was used to determine the diffusion coefficient along the DNA. The initial fast rise in the MSDs is due to the dynamic fluctuations in the DNA.

of the transverse coordinate (Fig. 3 B) were independent of time, except for a fast component with a rise time similar to the fast component in the longitudinal trajectories. The timescales (a few ms) and the amplitudes (~100 nm) of these fast components are due to the cyclic fluctuations of the DNAs in the flow/shear gradient plane. These fast fluctuations have been thoroughly characterized (34) and are similar to values we have previously reported (32).

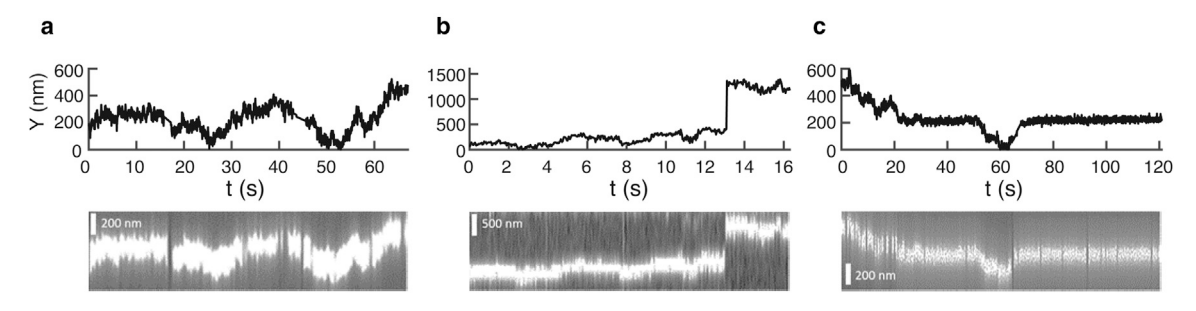


FIGURE 2 Kymographs and tracking of EcoRI<sup>E111Q</sup> molecules diffusing on DNA. (a) A single continuous diffusion trajectory is shown. (b) Two continuous trajectories are connected by a jumping event. (c) A continuous diffusion trajectory is interrupted by two pausing events.

To determine how much effect the flow in our experiment had on our results, we measured the average drift speed of the protein along the DNA. We found a salt-dependent drift speed that varied from 0.25 nm/s at 30 mM NaCl to 2.8 nm/s above 70 mM NaCl (Fig. S3). This drift accounts for 5–15% of the average length of DNA scanned per 1D search, indicating that the drift did not play a major role in the motion in our experiments.

We determined 1D diffusion coefficients from individual trajectories of the EcoRI position using linear fits to the MSD curves of the longitudinal coordinates (Fig. 3 A). To minimize the effect of the bias due to flow, we fit the MSDs to only the initial linear portion (typically 3–5 s) to determine the initial slope. To determine the relative contributions to the diffusion from sliding and hopping, we measured how the 1D diffusion coefficient varied with the salt concentration (Fig. 4). The diffusion coefficient was independent of salt concentration from 30 to 70 mM, with a mean of  $1.3 \times 10^{-3} \ \mu \text{m}^2/\text{s} \ (1.1 \times 10^4 \ \text{bp}^2/\text{s})$ , implying that sliding was the predominant mechanism of the search. Consistent with a sliding-based search, we observed very few jumps in the longitudinal position (5 out of 239 events, see example in Fig. 2 B). However, above 70 mM NaCl, the diffusion coefficient increased such that at 150 mM, it reached more than three times the low salt value, implying that hopping contributes more at these higher salt concentrations.

Each of the events identified as a jump consisted in a bound protein appearing near the dissociation point in the frame immediately after dissociation. These jumps are most likely due to the same protein reassociating after dissociation because the probability of another protein binding in the frame immediately after dissociation is negligible. We can estimate that probability in the following manner. We found the average occupation of a DNA (the total number of binding events divided by the total number of tethered DNAs in videos of length 120 s) to be 0.49. This implies an average binding

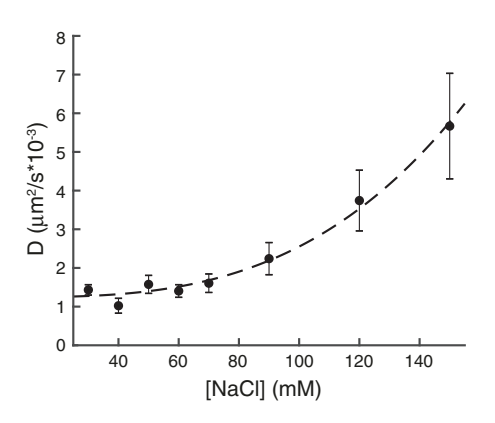


FIGURE 4 One-dimensional diffusion coefficient versus salt concentration. Shown is the mean of the diffusion coefficients at each salt concentration as determined by linear fits to the MSDs (135 events). The dashed curve is a fit to Eq. 1. Error bars represent the SE of the mean.

rate per DNA equal to  $0.49/120 \, \mathrm{s} = 0.0041 \, \mathrm{s}^{-1}$ . The probability of another protein binding in the exact frame after the first protein dissociates is this rate times the duration of a single frame (0.033 s). This probability is  $\sim 1.4 \times 10^{-4}$ . In 239 events, we would expect  $239 \times 1.4 \times 10^{-4} = \sim 0.03 << 1$  such events. We note that this is really an overestimate because for many events, we did not record the binding step, and hence, the association rate will actually be less than that calculated here. In addition, for many events, we did not see the dissociation, further reducing the expected number of such misidentified jumps.

The mean dwell times of the 1D diffusive interactions show a strong dependence on salt concentration (Fig. 5). Assuming the dissociation reaction follows the law of mass action, we fit the measured dwell times to a power law of the form A[Na<sup>+</sup>]<sup>-q</sup>, where A and q are fitting parameters. The exponent fits to a value of  $q=3.1\pm0.1$  and can be interpreted as the number of counterions released from the DNA upon nonspecific binding of the protein.

We also determined the 1D scan range (defined as the maximal minus minimal observed longitudinal coordinate for a single diffusion event) for each salt concentration. Fig. 6 shows this range as well as the expected root mean-square (RMS) displacement for each trajectory as calculated from the measured diffusion coefficients and dwell times. At [NaCl] <70 mM, the range is highly salt dependent because of the salt dependence of the dwell time. However, at a higher salt, the scan range and RMS displacement only depend weakly on salt because the reduced dwell time is compensated for by the increase in the diffusion coefficient.

A substantial number of trajectories (44%) showed pausing of EcoRI during 1D diffusion. Some trajectories showed the enzyme diffusing one dimensionally to the pause site, where it stalled upon reaching the site. In other trajectories, the protein could be seen leaving the pause site, diffusing away and then returning to pause once again

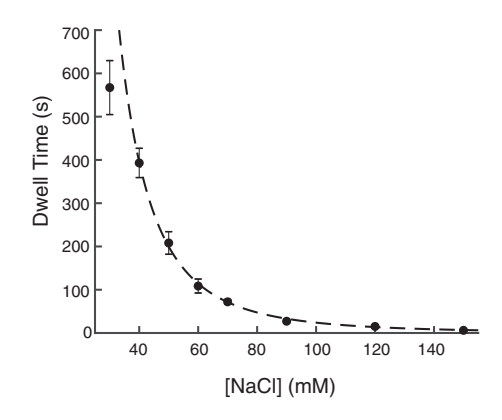


FIGURE 5 Mean dwell times of diffusing EcoRI<sup>E111Q</sup> versus salt concentration. The dwell time was determined as the time from initial appearance on the DNA until dissociation, indicated by the disappearance of the fluorescently labeled protein (135 events). The dashed curve is a fit to a power law (exponent =  $3.1 \pm 0.1$ ). Error bars represent the SE of the mean.

at the same (or indistinguishable nearby) site (Fig. 2 C). In yet other cases, the nonspecifically bound protein did not display any diffusion along the DNA during the entire data collection. Using the labeled cognate sites for reference, we were able to map the genomic locations of these pause sites and determine that many of them clustered into distinct regions of the DNA, indicating that EcoRI pauses at several specific noncognate sites in the  $\lambda$  genome. These observations led us to consider whether these pause sites could be EcoRI star sites. Star sites vary by a single basepair from the cognate sequence. High throughput sequencing methods have characterized star activity in whole bacterial genomes (31). We mapped out the location of the four most prevalent EcoRI star sites identified in (31) and compared these to our observed pause sites (see Fig. 7). The high correlation between the two distributions (p = $1.0 \times 10^{-3}$ ) indicates that EcoRI pauses preferentially at star sites.

### **DISCUSSION**

### The interaction of EcoRI with nonspecific DNA

In the presence of a single species of counterion, the nonspecific off rate is proportional to a power of the ion concentration with the exponent equal to the number of cations displaced upon protein binding. The crystal structure of EcoRI in complex with cognate DNA shows that the protein

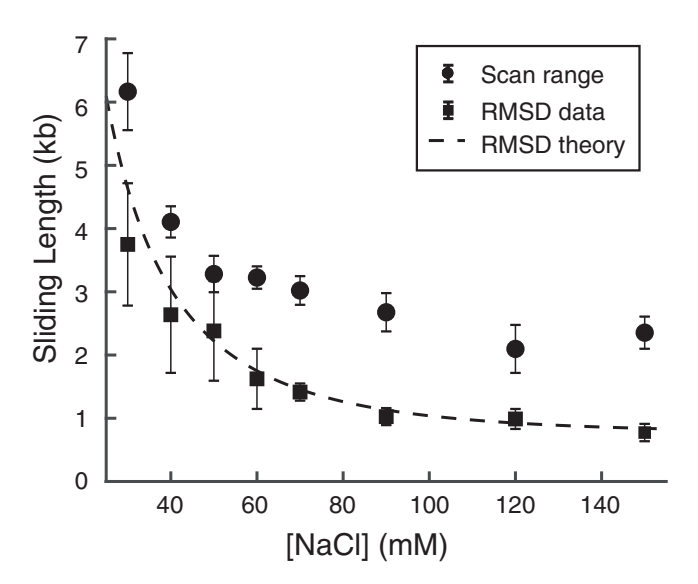


FIGURE 6 Mean scan range of diffusion events versus salt concentration. The scan range (solid circles) was calculated as the maximal length scanned in the 1D diffusion event (i.e., the maximal minus the minimal longitudinal coordinate in a single diffusion trajectory). Also plotted (solid squares) is the RMSD due solely to diffusion as calculated from the data shown in Figs. 4 and 5 ( $\Delta y = \sqrt{2D < t>}$ , where < t > is the mean dwell time, and D is the measured diffusion coefficient). The dashed curve is the theoretical RMSD from the fit of Eq. 1. Error bars represent the standard error of the mean.

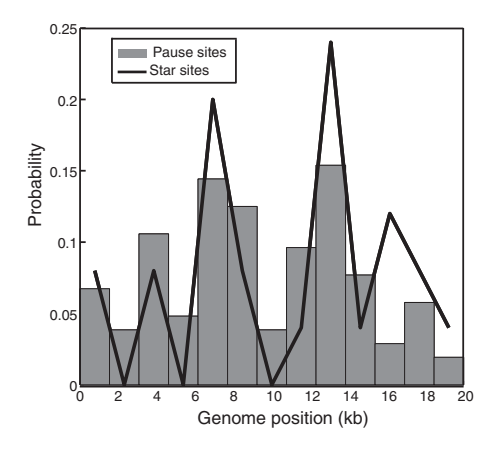


FIGURE 7 Comparison of observed pause sites and star sites. The probability of encountering a site is calculated as the number of sites in the region divided by the total number of sites. The distribution of pausing (104 events, shown in columns) and genomic star sites (solid line) show a high correlation (0.69). The probability of obtaining the observed correlation, assuming randomly distributed pause sites (p value), is  $1.0 \times 10^{-3}$ .

completely covers the six recognition bases, implying  $\sim$ 12 phosphate groups are blocked by the EcoRI footprint (27). Assuming an occupation of 0.76 of the phosphate groups by counterions (35), we expect a release of  $\sim$ 9 ions upon the formation of the specific complex. Multiple biochemical experiments that measured the salt dependence of the dissociation of EcoRI from its cognate site have shown an exponent of  $\sim 6$  (36–38), slightly lower than this estimate. However, to date, there has been no direct measurement of the salt dependency of the nonspecific off rate.

Our data shows that the nonspecific off rate scales with salt concentration with an exponent of 3.1  $\pm$  0.1 (Fig. 5), significantly less than that of the specific off rate ( $\sim$ 6). One complication of our analysis is that the interactions we observed are most likely made up of multiple cycles of sliding and hopping. This is because small hops cannot be distinguished from the dynamic fluctuations in the DNA. The mean dwell time we measure is  $t = t_S + t_H$ , where  $t_S$ is the mean time spent in sliding, and  $t_H$  is the mean time spent hopping. We first assume  $t_H$  is insignificant compared to  $t_S$ . This is sensible because the mean time per hop is controlled by the three-dimensional diffusion coefficient (15  $\mu$ m<sup>2</sup>/s from (32)), which is significantly greater than that of 1D diffusion. In addition, we do not expect the number of hops to greatly exceed the number of sliding events. In fact, equality of hopping and sliding events is consistent with the numerical results of DeSantis et al. (39) and is assumed in the scaling theory of Halford and Marko (40). Therefore,  $t \approx t_S = N_S \tau_S$ , where  $N_S$  is the number of sliding events per nonspecific interaction, and  $\tau_S$  is mean time per sliding event. We further assume that the number of sliding cycles will not depend strongly on salt. This is sensible because it only depends on the probability of recurrence once the protein has dissociated, a probability which is determined by the statistics of three-dimensional diffusion.

We note that these assumptions are consistent with the results of (39). Therefore, the scaling exponent, we determined, should reflect that of the intrinsic off rate from the sliding (nonspecifically bound) state. Our data implies that the nonspecific sliding state is significantly looser than the specific state, displacing roughly half the counterions displaced in the cognate recognition complex.

## Sliding and hopping both contribute to the 1D search

One-dimensional diffusion along DNA has frequently been characterized as sliding or hopping, depending on whether or not the diffusion coefficient displays a strong dependence on salt concentration. This follows naturally from the assumption that the protein-DNA nonspecific complex relies primarily on electrostatic interactions between protein and DNA backbone. Hence, hopping, which requires dissociation, will be enhanced as salt increases. Proteins such as hOGG1 (6), p52 (7), and T7 RNAP (16) have shown little if any dependence on salt and therefore have been classified as sliding. On the other hand, EcoRV (8) and UL42 (19) have displayed significant salt dependence and therefore have been identified as using a hopping mechanism. Proteins that encircle the DNA with a ring structure, such as sliding clamps, are also expected to have weak salt dependence, because their stability is primarily due to steric constraints, and to use a sliding mechanism. They also display significantly higher 1D diffusion coefficients (41). The relationship between salt dependence and diffusion mechanism is not always that simple. Recent work on TALE proteins has suggested that these proteins wrap loosely around the DNA interacting with several turns of the helix and show a strong salt dependence but relatively little hopping (42).

When both mechanisms contribute to 1D diffusion, the salt dependence of nonspecific dissociation will lead to a salt dependence of the relative contributions of sliding and hoping. Because of the faster hopping motion, the diffusion coefficient should increase as the sliding contribution decreases. In the case of EcoRI, our data shows two limits of behavior. Below 70 mM NaCl, sliding dominated diffusion results in a diffusion coefficient that is largely independent of salt. However, at higher salt concentrations, the relative contribution of hopping to sliding increases, thus resulting in the diffusion coefficient increasing with salt concentration. This behavior of EcoRI is in contrast to other proteins in the same class that have not shown this transition from predominantly sliding to mixed sliding/hopping diffusion. For example, the diffusion coefficient of EcoRV (8) was observed to increase with salt over the entire range examined (10-60 mM NaCl). In the cases of T7 RNAP (0-50 mM NaCl, (16)) and hOGG1 (10-100 mM NaCl, (6)), no salt dependence was observed. It is interesting to note that the behavior observed for UL42 (see Fig. 3 b in (19)) is somewhat similar to what we observe for EcoRI.

In general, the 1D diffusion coefficient  $D_I$  will be a weighted average of two diffusion coefficients (39):

$$D_1 = \frac{D_S t_S + D_H t_H}{t_S + t_H}. (1)$$

In this equation,  $D_S$  and  $D_H$  are the sliding and hopping diffusion coefficients, and  $t_S$  and  $t_H$  are the mean total time spent in sliding and hopping. The three factors  $t_H$ ,  $D_S$ , and  $D_H$  ( $\cong D_3$ , the three-dimensional diffusion coefficient) will only depend weakly on salt concentration. The only strong dependency on salt then is through the  $t_S$  term. When  $D_S t_S >> D_H t_H$  (at low salt),  $D_I$  is equal to  $D_S$ . At high salt, when  $t_S << t_H$ ,  $D_I$  will again be independent of salt and will be equal to  $D_H \cong D_3$ . This second limit may be unobservable because it may only apply at extremely high salt. At intermediate concentrations,  $D_I$  will depend strongly on salt. Assuming the dwell time of the protein on nonspecific DNA follows a power law of the form t  $\sim [\mathrm{Na}^+]^{-q}$ , the diffusion coefficient will scale with salt concentration  $\sim [\mathrm{salt}]^q$  in this intermediate regime.

To determine quantitatively the separate contributions of sliding and hopping, we have fit the above equation to our data (see Fig. 5). Using the fit from the dwell times for the  $t_S$  term, and assuming  $D_H = D_3$ , there are only two free parameters,  $D_S$  and  $t_H$ . The constant value for  $D_I$  that we observe at low salt determines  $D_S = (1.24 \pm 0.09) \times 10^{-3} \, \mu \text{m}^2/\text{s}$  $((1.07 \pm 0.08) \times 10^4 \text{ bp}^2/\text{s})$ , and the critical salt value when  $D_I$  begins to increase determines  $t_H = 1.7 \pm 0.4$  ms. This later value implies that EcoRI spends  $\sim$ 1.7 ms in hopping during each 1D scan (excluding pauses). Our data does not allow us to determine the number of hops nor the number of sliding events per scan. However, the fit to the model determines that sliding and hopping make equal contributions to the mean-squared displacement at a salt concentration of  $\sim$ 100 mM, in which the total RMS displacement due to diffusion is  $\sim$ 950 bp for each 1D scan.

As the salt concentration increases above the critical value ( $\sim 100$  mM NaCl), the hopping contribution ( $D_H t_H$ ) remains relatively constant as the sliding contribution  $(D_S t_S)$  reduces. This leads to an increase in the transparency because the hops remain the same size, but the regions of DNA probed during each sliding phase decrease, eventually becoming smaller than the hop step size. The scan range remains relatively constant in this limit (due primarily to the hopping). This is illustrated in our data (Fig. 6), which shows that the scan range depends weakly on salt above 80 mM. This increase in transparency has the effect of making the 1D search less compact at higher salt. Whereas at low salt, the search is conducted by redundant overlapping sliding events, at higher salt, each 1D scan is comprised of a set of shorter sliding events, each connected by a hop that leaves gaps of unvisited sites between each slide.

In contrast to EcoRV, whose critical salt concentration seems to be less than 10 mM (8), the critical concentration

for EcoRI is closer to physiological salt concentrations because of the longer dwell time of the nonspecifically bound EcoRI. This explains prior biochemical data that suggests that at 50 mM NaCl, EcoRI effectively searches all intervening DNA when translocating between two sites (43). At this salt concentration, transparency is low, and the protein executes a compact search of the DNA. For the proteins that show no salt dependence of diffusion, such as hOGG1, p53, and T7 RNAP, our model can accommodate these observations if we assume the critical salt concentration was higher than those explored experimentally.

A significant amount of biochemical characterization of the 1D search by DNA binding proteins has been carried out at low salt. At high salt, higher transparency will lead to reductions in search efficiency. At low salt, DNA binding proteins can use a "single hit" approach, in which a single nonspecific encounter can lead to target acquisition via a compact and thorough search. This can lead to specific on rates proportional to DNA length as has been observed for 2REs (2,11). It is unlikely that this limit is valid under physiological conditions for this class of proteins.

### Rotational coupling and the energy landscape of sliding

When the nonspecific complex is maintained through electrostatic interaction with the DNA backbone, diffusive translocation is expected to couple to rotation of the protein, significantly reducing  $D_S$  compared to the free three-dimensional diffusion coefficient,  $D_3$ . Consistent with this is the fact that sliding clamps (41), which form a ring around DNA, as well as TALE proteins (42), which wrap loosely about the double helix, show weak coupling between translocation and rotation as well as diffusion coefficients much closer to their three-dimensional values. Although rotational coupling has been directly observed in one case (23), in most cases, some form of rotational coupling theory is assumed and then used to explain the reduction of  $D_S$  compared to  $D_3$ . In addition, thermodynamic energy barriers to single basepair translocation can reduce  $D_S$  further. It has also been shown that disorder (or roughness) in the energy barriers, as well as randomness in the depths of the local nonspecific binding energy wells, can further slow diffusion (24,44).

Our data allows us to apply theories of rotation-coupled sliding directly to the sliding diffusion coefficient  $D_{\rm S}$ . Including both the theory of rotation-coupled sliding (21) as well as the effect of diffusion in a rough potential (45) leads to the following form for the sliding diffusion coefficient,

$$D_{S} = D_{3}e^{-\varepsilon/k_{B}T} \left\{ 1 + \frac{4}{3} \left( \frac{R}{b} \right)^{2} + \left( \frac{R_{OC}}{b} \right)^{2} \right\}^{-1}. \tag{2}$$

In this expression,  $D_3$  is the free three-dimensional diffusion coefficient, the exponential term is an Arrhenius factor with an activation energy of  $\varepsilon$  (the energy barrier between adjacent sites), and the final term in brackets represents the reduction due to rotational coupling. In the rotational coupling term, R is the hydrodynamic radius of the protein,  $R_{OC}$  is the distance of the center of the protein to the central axis of the DNA, and b is the pitch of the DNA (0.54 nm/rad). To determine the rotational coupling, we can use our previous measurement of the hydrodynamic radius of the QD-labeled EcoRI (13.7  $\pm$  0.4 nm, (32)) and estimate  $R_{OC} \cong 13.7 \pm 1.0$  nm. Assuming these values, the rotational coupling term leads to a reduction factor of  $1500 \times (\pm 9\%)$ . The observed reduction factor is 15/  $0.00124 = 12{,}100 \times (\pm 10\%)$ , which is significantly greater than what rotational coupling alone can explain. The further reduction  $(12,100/1500 = 8.1\times)$  can be explained by the presence of thermodynamic energy barriers separating adjacent nonspecific binding sites and can be taken into account using the Arrhenius term in Eq. 2. This method determines a characteristic energy barrier of  $ln(8.1) = 2.1 \pm 0.4$  k<sub>B</sub>T, a number comparable to that found for other DNA binding proteins (6-8). Roughness of the energy landscape (randomness in the activation energies) could be another factor in the reduction of the diffusion coefficient. In a rough landscape, the average energy barrier will be less than the 2.1 k<sub>B</sub>T, which we determined here. The additional reduction in the diffusion coefficient will arise from randomness in the binding energies and barrier heights. However, our data does not allow us to independently determine the roughness parameter.

### Sequence-dependent pausing during a 1D search

Sequence-dependent pausing of DNA binding proteins during a 1D target search is poorly characterized. Kinetic data on association rates of EcoRI using DNAs containing star sites has been interpreted as implying that EcoRI pauses at these star sites for up to 20 s in 50 mM NaCl (43). Through direct imaging of EcoRI, we observe that it can remain bound to nonspecific sites for many minutes. These long pauses likely result from multiple unobserved small excursions and returns to the star site. We can assume the minimal distance the protein must diffuse before we can identify an excursion is one half the root mean-square deviation (RMSD) dynamic fluctuations in the DNA. This is  $\sim$ 200 bp as determined from the y intercept in Fig. 3 B. This value is consistent with the track shown in Fig. 2 C. which shows a just detectable excursion from the pause site at  $\sim 30$  s with an amplitude of  $\sim 200$  bp. Assuming the protein making the excursion is only sliding and starts from a nonspecific binding site displaced a single basepair from the pause site, this implies an escape probability of  $\sim$ 0.5%. The observed pauses are then composed of multiple "micropause" events, each linked by a short excursion and return. In the biochemical experiments in (43), the cognate site was less than 10 bp from the star site, and hence,

recurrence before specific association with the target site was much less likely. This picture agrees with the very long duration of the pauses we observed, many in excess of 20 min.

A model of the paused state has been proposed based on crystal structures of BstYI (29). In complex with star DNA, only one monomer of BstYI reaches into the major groove to make specific contacts, whereas the other monomer is rotated out and can only make nonspecific interactions. This mode of binding (termed "hemispecific" by the authors of (29)) suggests widely distributed pauses should occur at all sites that contain a single half cognate site. The observed distribution of EcoRI pausing shows enhancement at star sites. To reach the cognate-like interaction points in the noncognate half of the star site, EcoRI must adopt a more closed conformation, similar to the specific binding mode.

### A model of the 1D search by EcoRI

The above considerations suggest a model for sliding in which the protein adopts one of two types of interactions with noncognate DNA (see Fig. 8). In the nonspecific mode, the protein is positioned in a symmetric manner in the major groove and makes no specific contacts, similar to what has been observed for BamHI (28). Such an interaction is consistent with rapid translocation to neighboring sites and would lead to a uniform binding energy surface. In the hemispecific mode (analogous to the BstYI star structure), the protein is rotated, bringing one monomer into contact with the major groove in which it has access to specific contacts in a potential half site. Importantly, the nonspecific and hemispecific modes can rapidly interconvert because they are principally related by a rigid body rotation of the protein. Short pauses occur when target-like interactions with the probed half site stabilize the protein-DNA complex. From this short pause state, further conformational changes (which can involve both the closing of the protein dimer and the bending and opening of the major groove) occur that bring the opposite binding site in the protein into contact with the remaining half site. Cognate-like interactions in the sec-

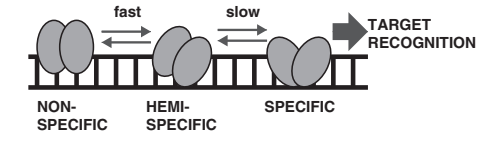


FIGURE 8 A model for a 1D search of DNA. In a 1D search, the protein rapidly intraconverts between the nonspecific binding mode and the hemispecific mode as it slides. Slower transitions to the specific mode of binding (which requires substantial conformational change) are more likely when cognate-like interactions in a half site stabilize the hemispecific binding mode. Target recognition, and subsequent catalysis, is only possible after the specific mode of binding is achieved.

ond half site will necessarily further stabilize the recognition complex, leading to a longer duration pause. It is these longer, sequence-dependent pause states that we observe because the shorter pauses are likely too fast to detect with our time resolution ( $\sim$ 30 ms). Once stabilized, the specific mode of binding can then lead to target recognition and subsequent hydrolysis of the phosphodiester bond

We note here that the recent model of asymmetric sliding (46) might also explain our observations. Coarsegrained molecular dynamics simulations suggest that dimeric proteins can slide in two modes: a symmetric slow mode, in which both monomers interact closely with the DNA, and an asymmetric faster mode, in which only one closely interacts with the DNA. This is distinct from the model we propose, in which the hemispecific binding mode does not slide. Higher salt might stabilize the asymmetric mode relative to the symmetric by increasing the off rate of the monomer, thus leading to faster diffusion at high salt. This explanation has the feature that hemispecific binding might naturally occur during asymmetric sliding. However, the salt dependence of the asymmetric sliding was shown in (46) to depend on which protein was simulated. For the restriction endonucleases examined (which included EcoRI), the asymmetric mode was destabilized at higher salt. Additionally, we saw no salt dependence on pausing, which would be expected if the pausing resulted from a saltdependent asymmetric mode of sliding.

In contrast to theories that require kinetic preselection, our model implies a relatively uniform nonspecific energy landscape. In this way, the protein can rapidly search nonspecific DNA and limit the occurrence of the specific binding mode to sites that are at least "half right." This suggests a solution to the speed/stability paradox similar to that of Levinthal's paradox of protein folding, in which the protein does not sample all possible folded conformations but proceeds through a specific set of intermediate states. The short pause state (due to hemispecific binding) as well as the longer pause state (with its more significant conformational changes) are then necessary intermediates that must occur before the formation of the protein-target recognition complex.

In summary, we have shown that a model that includes both hopping and sliding can explain quantitatively the salt dependence of diffusion that we observe. This model allows us to calculate quantitatively the separate contributions of each mechanism. Furthermore, we have shown that the theory of rotational coupling in a rough energy landscape can explain the sliding diffusion coefficient we have measured. We have also reported the presence of pausing in the 1D search and shown that these pause sites map onto genomic star sites. A model of a 1D search that includes a hemispecific binding mode can explain the role of these pauses in the search strategy.

#### **SUPPORTING MATERIAL**

Supporting Material can be found online at https://doi.org/10.1016/j.bpj. 2019.04.035.

### **AUTHOR CONTRIBUTIONS**

S.C.P. performed experiments, analyzed data, and wrote article. J.J.L. designed research and wrote article. A.C.P. designed research, analyzed data, and wrote article.

### **ACKNOWLEDGMENTS**

We thank HyeongJun Kim for assistance in preparing the QD-labeled protein.

Support for this work also comes from a National Institutes of Health grant R01GM115487 (to J.J.L.) and the National Science Foundation Research in Undergraduate Institutions Award MCB-1715317 (to A.C.P.).

### **REFERENCES**

- Winter, R. B., O. G. Berg, and P. H. von Hippel. 1981. Diffusion-driven mechanisms of protein translocation on nucleic acids. 3. The *Escheri*chia coli lac repressor-operator interaction: kinetic measurements and conclusions. *Biochemistry*. 20:6961–6977.
- Terry, B. J., W. E. Jack, and P. Modrich. 1985. Facilitated diffusion during catalysis by EcoRI endonuclease. Nonspecific interactions in EcoRI catalysis. *J. Biol. Chem.* 260:13130–13137.
- Gowers, D. M., G. G. Wilson, and S. E. Halford. 2005. Measurement of the contributions of 1D and 3D pathways to the translocation of a protein along DNA. *Proc. Natl. Acad. Sci. USA.* 102:15883–15888.
- Wang, Y. M., R. H. Austin, and E. C. Cox. 2006. Single molecule measurements of repressor protein 1D diffusion on DNA. *Phys. Rev. Lett.* 97:048302.
- Granéli, A., C. C. Yeykal, ..., E. C. Greene. 2006. Long-distance lateral diffusion of human Rad51 on double-stranded DNA. *Proc. Natl. Acad.* Sci. USA. 103:1221–1226.
- Blainey, P. C., A. M. van Oijen, ..., X. S. Xie. 2006. A base-excision DNA-repair protein finds intrahelical lesion bases by fast sliding in contact with DNA. *Proc. Natl. Acad. Sci. USA*. 103:5752–5757.
- Tafvizi, A., F. Huang, ..., A. M. van Oijen. 2008. Tumor suppressor p53 slides on DNA with low friction and high stability. *Biophys. J.* 95:L01– L03.
- Bonnet, I., A. Biebricher, ..., P. Desbiolles. 2008. Sliding and jumping of single EcoRV restriction enzymes on non-cognate DNA. *Nucleic Acids Res.* 36:4118–4127.
- Tafvizi, A., F. Huang, ..., A. M. van Oijen. 2011. A single-molecule characterization of p53 search on DNA. *Proc. Natl. Acad. Sci. USA*. 108:563–568.
- Iwahara, J., and Y. Levy. 2013. Speed-stability paradox in DNA-scanning by zinc-finger proteins. *Transcription*. 4:58–61.
- Ehbrecht, H. J., A. Pingoud, ..., C. Gualerzi. 1985. Linear diffusion of restriction endonucleases on DNA. J. Biol. Chem. 260:6160–6166.
- van den Broek, B., M. A. Lomholt, ..., G. J. Wuite. 2008. How DNA coiling enhances target localization by proteins. *Proc. Natl. Acad. Sci. USA*. 105:15738–15742.
- Gambino, S., B. Mousley, ..., A. C. Price. 2016. A single molecule assay for measuring site-specific DNA cleavage. *Anal. Biochem.* 495:3–5.
- Pingoud, A., M. Fuxreiter, ..., W. Wende. 2005. Type II restriction endonucleases: structure and mechanism. *Cell. Mol. Life Sci.* 62:685–707.

- Berg, O. G., R. B. Winter, and P. H. von Hippel. 1981. Diffusion-driven mechanisms of protein translocation on nucleic acids. 1. Models and theory. *Biochemistry*. 20:6929–6948.
- Kim, J. H., and R. G. Larson. 2007. Single-molecule analysis of 1D diffusion and transcription elongation of T7 RNA polymerase along individual stretched DNA molecules. *Nucleic Acids Res.* 35:3848–3858.
- Redner, S. 2001. A Guide to First-Passage Processes. Cambridge University Press, Cambridge, UK.
- De Gennes, P. 1982. Kinetics of diffusion-controlled processes in dense polymer systems. I. Nonentangled regimes. *J. Chem. Phys.* 76:3316– 3321
- Komazin-Meredith, G., R. Mirchev, ..., D. M. Coen. 2008. Hopping of a processivity factor on DNA revealed by single-molecule assays of diffusion. *Proc. Natl. Acad. Sci. USA*. 105:10721–10726.
- Schurr, J. M. 1979. The one-dimensional diffusion coefficient of proteins absorbed on DNA. Hydrodynamic considerations. *Biophys. Chem.* 9:413–414.
- Bagchi, B., P. C. Blainey, and X. S. Xie. 2008. Diffusion constant of a nonspecifically bound protein undergoing curvilinear motion along DNA. J. Phys. Chem. B. 112:6282–6284.
- 22. Blainey, P. C., G. Luo, ..., X. S. Xie. 2009. Nonspecifically bound proteins spin while diffusing along DNA. *Nat. Struct. Mol. Biol.* 16:1224–1229
- Sakata-Sogawa, K., and N. Shimamoto. 2004. RNA polymerase can track a DNA groove during promoter search. *Proc. Natl. Acad. Sci.* USA. 101:14731–14735.
- Slutsky, M., and L. A. Mirny. 2004. Kinetics of protein-DNA interaction: facilitated target location in sequence-dependent potential. *Bio-phys. J.* 87:4021–4035.
- Veksler, A., and A. B. Kolomeisky. 2013. Speed-selectivity paradox in the protein search for targets on DNA: is it real or not? *J. Phys. Chem.* B. 117:12695–12701.
- Yu, S., S. Wang, and R. G. Larson. 2013. Proteins searching for their target on DNA by one-dimensional diffusion: overcoming the "speed-stability" paradox. J. Biol. Phys. 39:565–586.
- Kim, Y. C., J. C. Grable, ..., J. M. Rosenberg. 1990. Refinement of Eco RI endonuclease crystal structure: a revised protein chain tracing. Science. 249:1307–1309.
- Viadiu, H., and A. K. Aggarwal. 2000. Structure of BamHI bound to nonspecific DNA: a model for DNA sliding. *Mol. Cell.* 5:889–895.
- **29.** Townson, S. A., J. C. Samuelson, ..., A. K. Aggarwal. 2007. BstYI bound to noncognate DNA reveals a "hemispecific" complex: implications for DNA scanning. *Structure*. 15:449–459.
- Graham, T. G., X. Wang, ..., J. J. Loparo. 2014. ParB spreading requires DNA bridging. Genes Dev. 28:1228–1238.
- Kamps-Hughes, N., A. Quimby, ..., E. A. Johnson. 2013. Massively parallel characterization of restriction endonucleases. *Nucleic Acids Res.* 41:e119.
- Price, A. C., K. R. Pilkiewicz, ..., J. J. Loparo. 2015. DNA motion capture reveals the mechanical properties of DNA at the mesoscale. *Biophys. J.* 108:2532–2540.
- 33. Doyle, P. S., B. Ladoux, and J. L. Viovy. 2000. Dynamics of a tethered polymer in shear flow. *Phys. Rev. Lett.* 84:4769–4772.
- Lueth, C. A., and E. S. Shaqfeh. 2009. Experimental and numerical studies of tethered DNA shear dynamics in the flow-gradient plane. *Macromolecules*. 42:9170–9182.
- Lohman, T. M. 1986. Kinetics of protein-nucleic acid interactions: use of salt effects to probe mechanisms of interaction. CRC Crit. Rev. Biochem. 19:191–245.
- Lesser, D. R., M. R. Kurpiewski, ..., L. Jen-Jacobson. 1993. Facilitated distortion of the DNA site enhances EcoRI endonuclease-DNA recognition. *Proc. Natl. Acad. Sci. USA*. 90:7548–7552.
- Sidorova, N. Y., and D. C. Rau. 2001. Linkage of EcoRI dissociation from its specific DNA recognition site to water activity, salt

- concentration, and pH: separating their roles in specific and non-specific binding. *J. Mol. Biol.* 310:801–816.
- Sidorova, N. Y., T. Scott, and D. C. Rau. 2013. DNA concentrationdependent dissociation of EcoRI: direct transfer or reaction during hopping. *Biophys. J.* 104:1296–1303.
- DeSantis, M. C., J. L. Li, and Y. M. Wang. 2011. Protein sliding and hopping kinetics on DNA. *Phys. Rev. E Stat. Nonlin. Soft Matter Phys.* 83:021907.
- Halford, S. E., and J. F. Marko. 2004. How do site-specific DNA-binding proteins find their targets? *Nucleic Acids Res.* 32:3040–3052.
- Daitchman, D., H. M. Greenblatt, and Y. Levy. 2018. Diffusion of ringshaped proteins along DNA: case study of sliding clamps. *Nucleic Acids Res.* 46:5935–5949.

- Cuculis, L., Z. Abil, ..., C. M. Schroeder. 2016. TALE proteins search DNA using a rotationally decoupled mechanism. *Nat. Chem. Biol.* 12:831–837.
- Jeltsch, A., J. Alves, ..., A. Pingoud. 1994. Pausing of the restriction endonuclease EcoRI during linear diffusion on DNA. *Biochemistry*. 33:10215–10219.
- 44. Hu, T., and B. I. Shklovskii. 2006. How does a protein search for the specific site on DNA: the role of disorder. *Phys. Rev. E Stat. Nonlin. Soft Matter Phys.* 74:021903.
- 45. Zwanzig, R. 1988. Diffusion in a rough potential. *Proc. Natl. Acad. Sci. USA*. 85:2029–2030.
- **46.** Khazanov, N., A. Marcovitz, and Y. Levy. 2013. Asymmetric DNA-search dynamics by symmetric dimeric proteins. *Biochemistry*. 52:5335–5344.